Supporting Information

For

Electrocatalytic oxidation of n-propanol to produce propionic acid by an electrocatalytic membrane reactor

Jiao Li,[a] Jianxin Li,[a] Hong Wang,[a] Bowen Cheng,[a] Benqiao He,[a] Feng Yan,[a] Yang Yang,[a] Wenshan Guo[b] and Huu Hao Ngo[b]*

[a]State Key Laboratory of Hollow Fiber Membrane Materials and Processes, School of Materials Science and Engineering, Tianjin Polytechnic University, Tianjin 300387, P. R. China

[b]Centre for Technology in Water and Wastewater, School of Civil and Environmental Engineering, University of Technology Sydney, PO Box 123 Broadway, NSW 2007, Australia

*E-mail: jxli0288@yahoo.com.cn or jxli@tjpu.edu.cn (J. Li);

Table of Contents:

Experimental Section

Preparation and characterization of MnO_2/Ti membrane. Commercially available tubular porous conductive Ti membrane with an average pore size of 10.8 μm, ID/OD=19 mm/28.5 mm and specific surface area of 230 m^2/g was used as the substrate. The membrane with the filtration area of 52.2 cm^2 was first pretreated in 10 wt.% boiled oxalic acid solution for 1 h, then was cleaned with large amounts of deionized water and dried at room temperature. Secondly, the membrane was dipped into 50 wt.% $Mn(NO_3)_2$ solution for 0.5 h and then dried at room temperature. Afterwards, the treated membrane was placed in a tube furnace to sinter at the designed temperature for 2 h. Finally, a functional nano-MnO_2 loading Ti membrane (MnO_2/Ti electrocatalytic membrane) was obtained with the MnO_2 loading of 3.6 wt.% (The weight of the substrate is 69.26 g). The morphologies and structures of the membrane were observed by FESEM (Hitachi S-4800, Japan), EDS (GENESIS 60S), HRTEM (JEM-2100) and XPS (Thermofisher K-Alpha). XRD patterns were obtained using D/MAX-2500 (Cu K_α λ= 1.5406Å). EIS was performed using a Electrochemical workstation (ZAHNER Zennium).

Electrochemical synthesis of propionic acid from n-propanol. Propionic acid and propanal would appear in both feed and permeate during the synthesis of propionic acid from n-propanol by the ECMR.

The conversion for reactant n-propanol within a period of reaction time can be described as Equation (S1):[S1]

$$\%\ \text{Conversion of n-propanol} = \frac{(x_{F-OH}\cdot V_F)-(x_{P-OH}\cdot V_P)-(x_{R-OH}\cdot V_R)}{(x_{F-OH}\cdot V_F)-(x_{R-OH}\cdot V_R)}\times 100\% \qquad \text{(S1)}$$

The selectivity for product - propionic acid in both feed and permeate within a period of reaction time can be expressed as Equation (S2):[S2]

$$\%\ \text{Selectivity of propionic acid} = \frac{(x_{P-COOH} \cdot V_P) + (x_{R-COOH} \cdot V_R)}{(x_{F-OH} \cdot V_F) - (x_{P-OH} \cdot V_P) - (x_{R-OH} \cdot V_R)} \times 100\% \qquad \text{(S2)}$$

where x_{F-OH} is the initial molar fraction of n-propanol in the feed (mmol/L), V_F is the initial volume of the feed (L); x_{P-OH} and x_{R-OH} are the molar fraction of n-propanol in permeate and in the residual solution in the feed tank (mmol/L); V_P and V_R are the volume of the permeate and the residual solution in the feed tank (L); x_{P-COOH} and x_{R-COOH} are the molar fraction of propionic acid in the permeate and the residual solution (mmol/L).

The reactant, the intermediates and the product were analyzed with GC-MS system (Agilent 6890N-5975C) equipped with a HP-5MS column (30.0 m × 0.25 mm). The concentration of the targeted components was determined by GC (Agilent GC-6890N) with a FFAP column (30.0 m × 0.25 mm).

Table S1 The conversion of n-propanol at different working potential.

The working potential (V)	2.56	2.67	2.78	2.86	3.12
The conversion of n-propanol (%)	66.55	70.8	77.1	73.2	71.8

The operation voltage was 2.5 V and the reaction temperature was 25 °C at 22.55 min of residence time, respectively. It was found from Table S1 that the conversion of n-propanol increased from 66.55% to 77.1% with the working potential increased from 2.56 V to 2.78 V , and then decreased to 71.8% when the working potential further increased to 3.12 V.

It also could be seen from the above experiment that the operating current also increased from 61 mA to 120 mA with the increase of the potential from 2.56 V to 2.78 V. The larger current generated between anode and the cathode would produce the more electrogenerated intermediate,[S3] leading to the increasing conversion. However, when the operating potential was more than 2.78 V, water decomposition would compete with n-propanol oxidation. As a result, some of the applied energy is consumed by water decomposition instead of the oxidation of n-propanol, which resulted in a lower conversion. Therefore, the working potential of 2.8 V was chose in this paper according to the above observations.

Table S2 a) The qualitative analysis of n-propanol in the feed

PK	Area Pct	Library/ID
1	1.817	1-Propanol

Table S2 b) Composition analysis of the permeate in the ECMR operation

PK	Area Pct	Library/ID
1	1.813	1-Propanol
2	1.597	Propanal
3	4.065	Propionic acid
4	4.493	Propinoic acid, propyl ester

Table S3 The carbon balance before and after electrocatalytic reaction at different residence time and temperature.

Residence time (min)	Reaction temperature (°C)	n_{OH-0} (mmol)	n_{OH-1} (mmol)	n_{COOH-1} (mmol)	n_{CHO-1} (mmol)	Δn (mmol)
0	25	166.22	138.86	4.19	1.34	21.83
0.54	25	156.04	129.93	9.23	11.55	5.33
3.22	25	152.08	110	16.64	16.58	8.86
5.84	25	150.77	96.81	22.09	22.14	9.73
11.83	25	165.17	94.57	37.68	21.83	11.09
15.47	25	165.62	80.43	49.93	22.71	12.55
18.68	25	150.92	60.02	61.41	16.16	13.33
22.55	25	167.66	38.18	110.58	9.78	9.12
22.55	50	163.57	2.59	157.5	2.63	0.85

n_{OH-0} was the amount of n-propanol before reaction (mmol); n_{OH-1} was the amount of n-propanol in the feed and permeate after the reaction time 75 min (mmol); n_{COOH-1} and n_{CHO-1} were the amount of propionic acid and propanal in the feed and permeate after the reaction time 75 min (mmol).

Δn can be described as the following equation:

$$\Delta n = n_{OH-0} - n_{OH-1} - n_{COOH-1} - n_{CHO-1} \quad \text{(S1)}$$

The value of Δn represented the amount of n-propanol mineralized completely into carbon dioxide and water and/or used to react with acid to produce propyl propionate by esterification during the ECMR operation. It can be found from Table S2 that the value of Δn at residence time 0 min was 21.83, which was larger than those obtained at other residence times (0.85~13.33). This result indicated that propionic acid can be easily oxidized to CO_2 and H_2O at the residence time of 0 min owning to the limit of mass transfer.

Table S4 The instantaneous flow rate at different residence time.

Residence time (min)	Instantaneous permeate (mL/min)
0.54	5.00
3.22	0.83
5.84	0.46
11.83	0.23
15.47	0.17
18.68	0.14
22.55	0.12

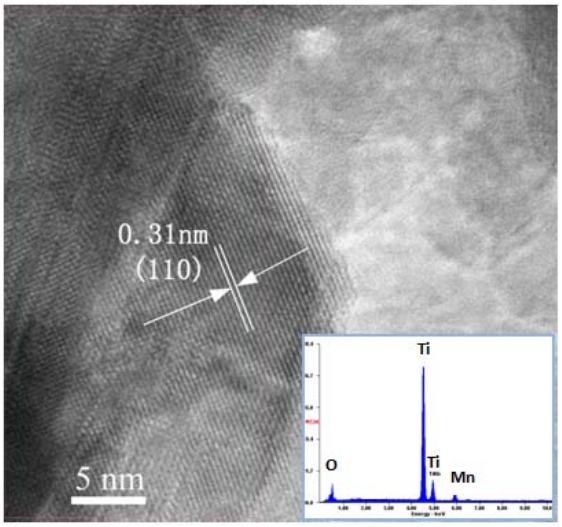

Fig.S1 High-resolution TEM images of MnO_2 power.

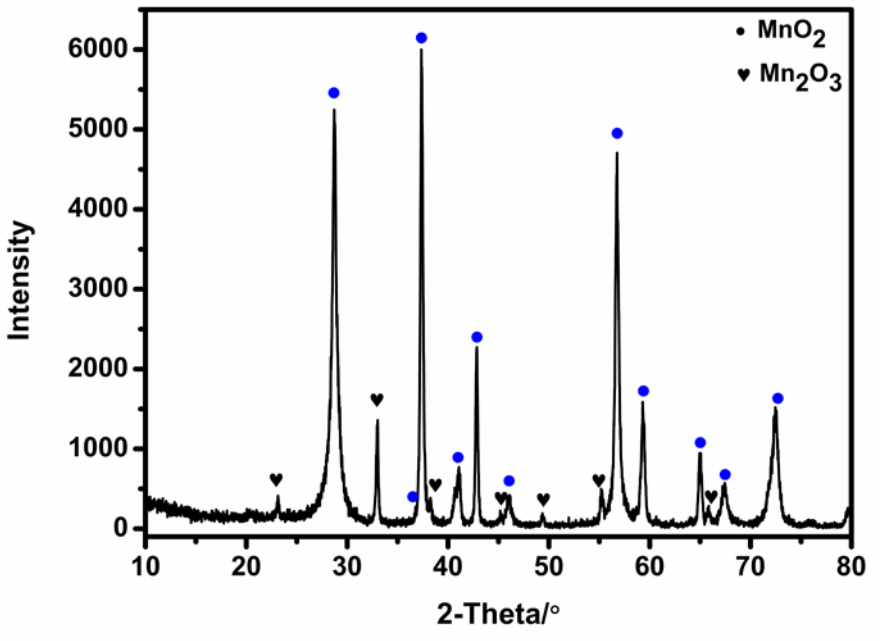

Figure S2-1. X-ray diffraction pattern of the synthesized MnO_2 obtained at 350°C.

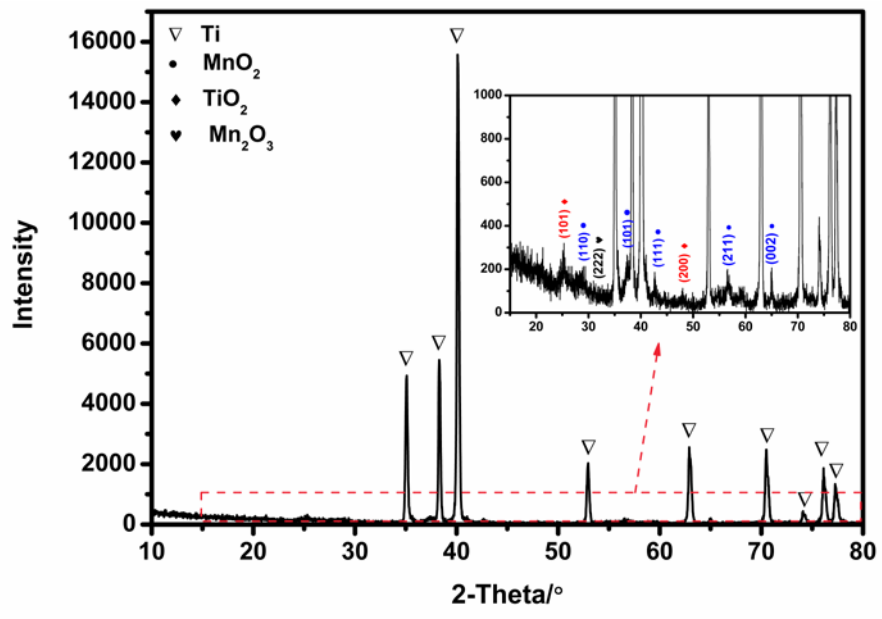

Figure S2-2. X-ray diffraction pattern of the MnO_2/Ti membrane.

As shown in Figure S1-1, the representative peaks of MnO_2 particles observed located at 2θ=28.68°, 37.33°, 41.01°, 42.82°, 46.08°, 56.65°, 59.37°, 64.83° and 72.38°, which were characteristic peaks of the pyrolusite-MnO_2 crystals (JCPDS No. 24-0735). It also can be seen from Figure S1-1 that some weak small diffraction peaks appeared at 2θ=23.13°, 32.95°, 38.23°, 45.18°, 49.35°, 55.189° and 65.806°, which can be indexed to the Bixbyite-C-Mn_2O_3 crystals (JCPDS No. 41-1442). The average

crystal size of the obtained particles was calculated by Scherer's formula: $D=k\lambda/\beta\cos\theta$, where D is the average crystal diameter, k is a constant of 0.89, λ is the radiation wavelength of 0.154 nm, β is full width at half-maximum of diffraction peak, and θ is the Bragg angel of approximately 22.7 nm. X-ray diffraction pattern of the MnO_2 loading Ti (MnO_2/Ti) electrocatalytic membrane was also presented in Figure S1-2. Except for the obvious peaks of Ti crystals, there were also corresponding peaks of the pyrolusite-MnO_2 crystals and the Bixbyite-C-Mn_2O_3 crystals. In addition, the diffraction peaks of TiO_2 crystals observed at $2\theta=25.28°$, 48.05°, were identified to the anatase phase (JCPDS No. 21-1272).

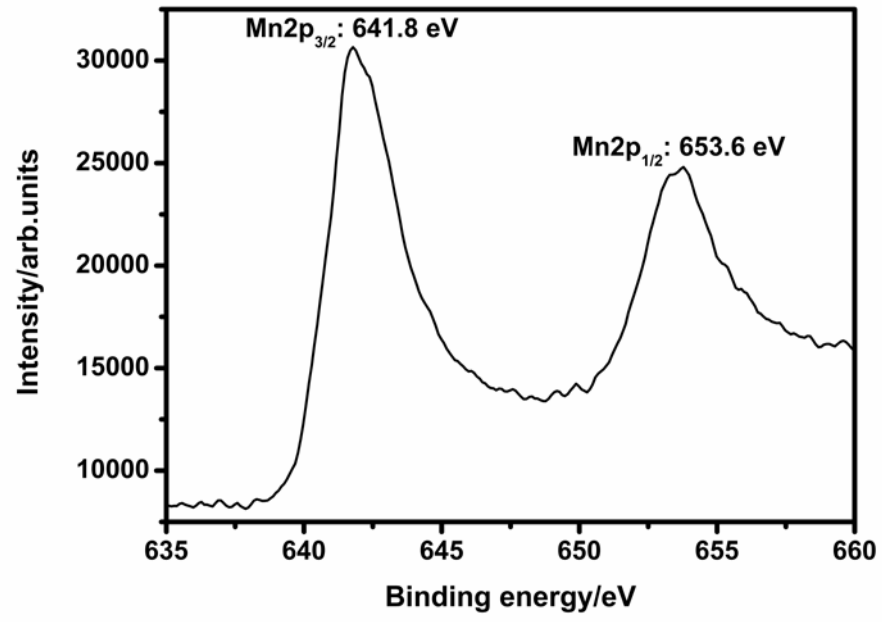

Figure S3. XPS spectra of the MnO_2/Ti membrane. The binding energy of Mn $2p_{3/2}$ and $2p_{1/2}$ were 641.8 and 653.6 eV, respectively. The different binding energy between Mn $2p_{3/2}$ and $2p_{1/2}$ was 11.8 eV. It revealed that the valence state of Mn was 4+. The results obtained are in good agreement with the reported data of Mn $2p_{3/2}$ and $2p_{1/2}$ in MnO_2.[S4]

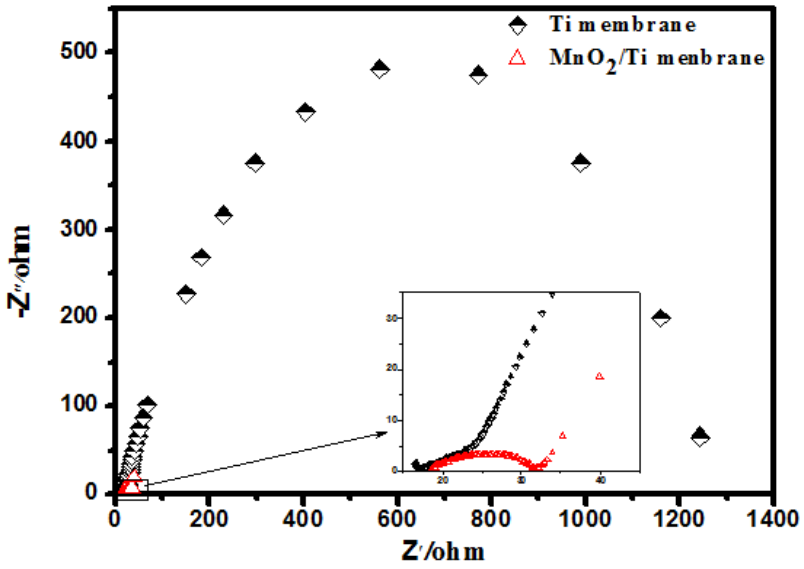

Figure S4. Electrochemical impedence spectra (EIS) of Ti and MnO_2/Ti membrane. It depicts the electrochemical performance of the MnO_2/Ti membrane measured by EIS (amplitude of 10 mV, frequency range of 0.5 mHz to 100 kHz, in 0.1 M H_2SO_4 solution). It can be seen from Figure S3 that the EIS Nyquist plot included the semicircle and straight-line parts. The charge-transfer resistance (RCT) was equal to the diameter of the semicircle on the EIS Nynquist plot. The smaller the arc radius of an EIS nyquist plot, the higher the efficiency of charge separation was. The radius of semicircle in the high frequency range obtained from the MnO_2/Ti electrode was 2.36 $\Omega \cdot cm^{-2}$, which was much smaller than that of the Ti membrane (10.27 $\Omega \cdot cm^{-2}$). This result suggested that the enhanced electronic conductivity of MnO_2/Ti electrode was attributed to the special energy band structure of MnO_2 crystals.

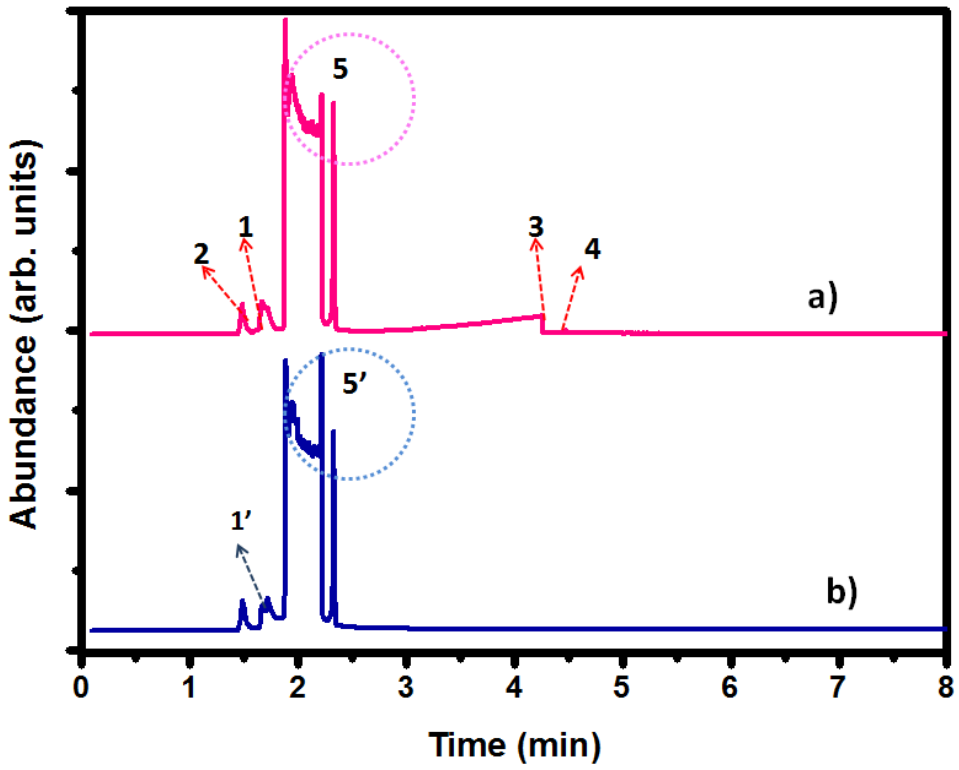

Figure S5. Gas chromatography-mass spectrometer (GC-MS) analysis: a) permeate; b) n-propanol in the feed. Methylene chloride and trichloromethane also appeared in the feed and the permeate (peaks 5 and 5') because they were used as the cleaner and extraction agent, respectively. According to Table S1b, the feed only had n-propanol. Propanal, propionic acid and a small amount of propyl propionate except for n-propanol appeared in the permeate were the product, intermediate product and by-product of electrocatalytic oxidation of n-propanol, respectively (Table S1a).

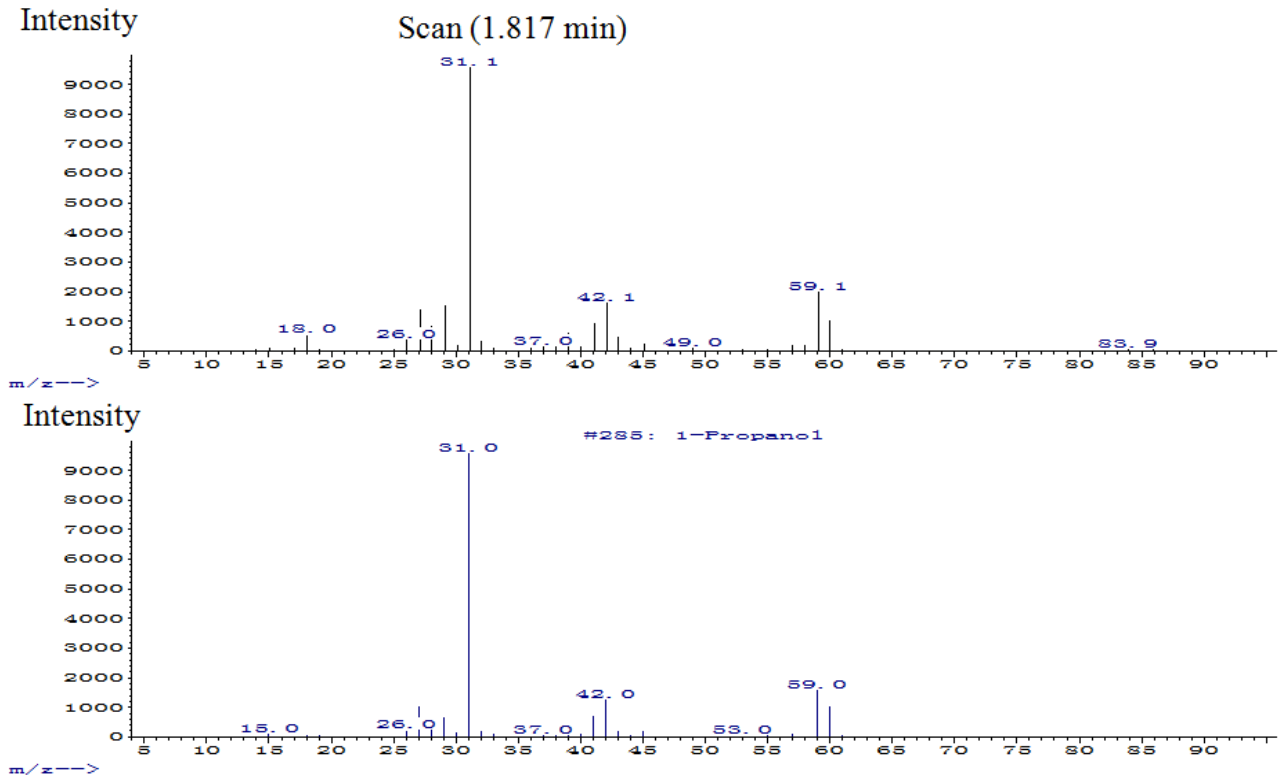

Figure S5-1. The Mass Spectra of n-paopanol in the feed.

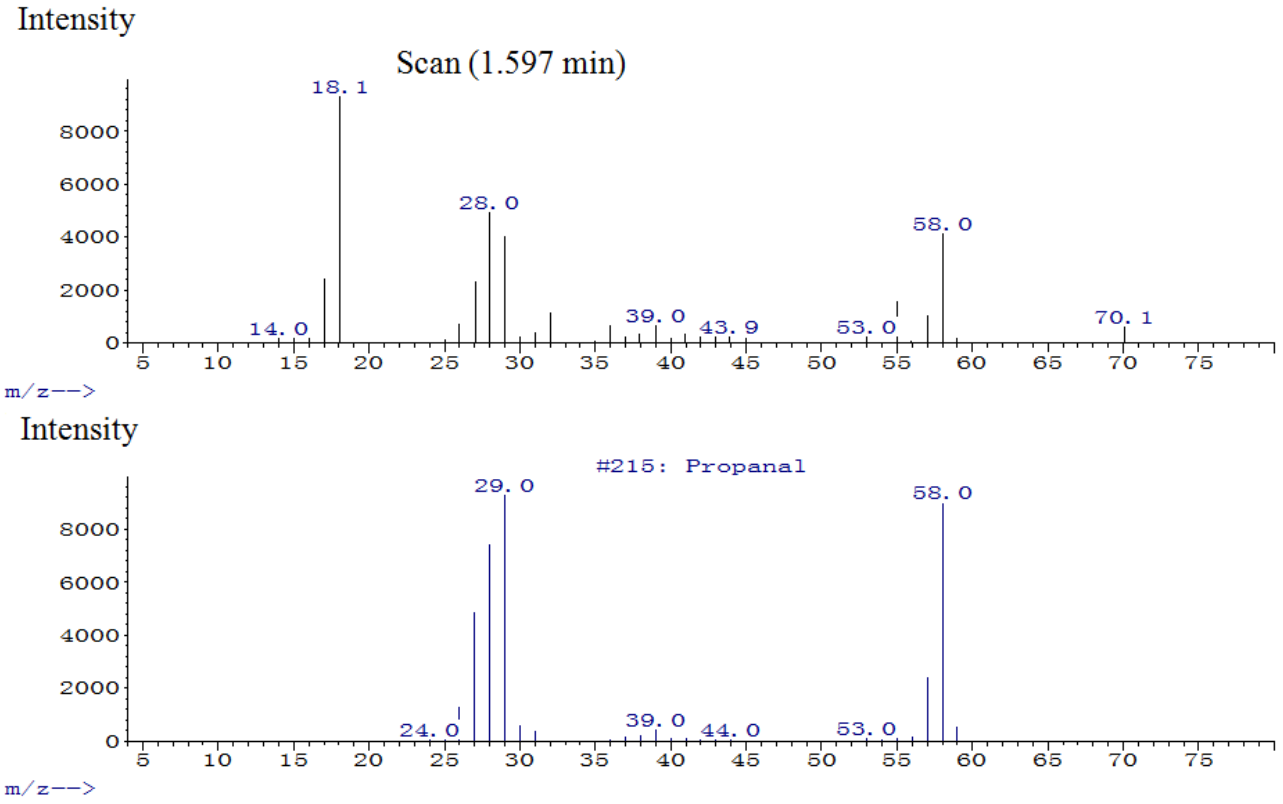

Figure S5-2. The Mass Spectra of propanal in the permeate.

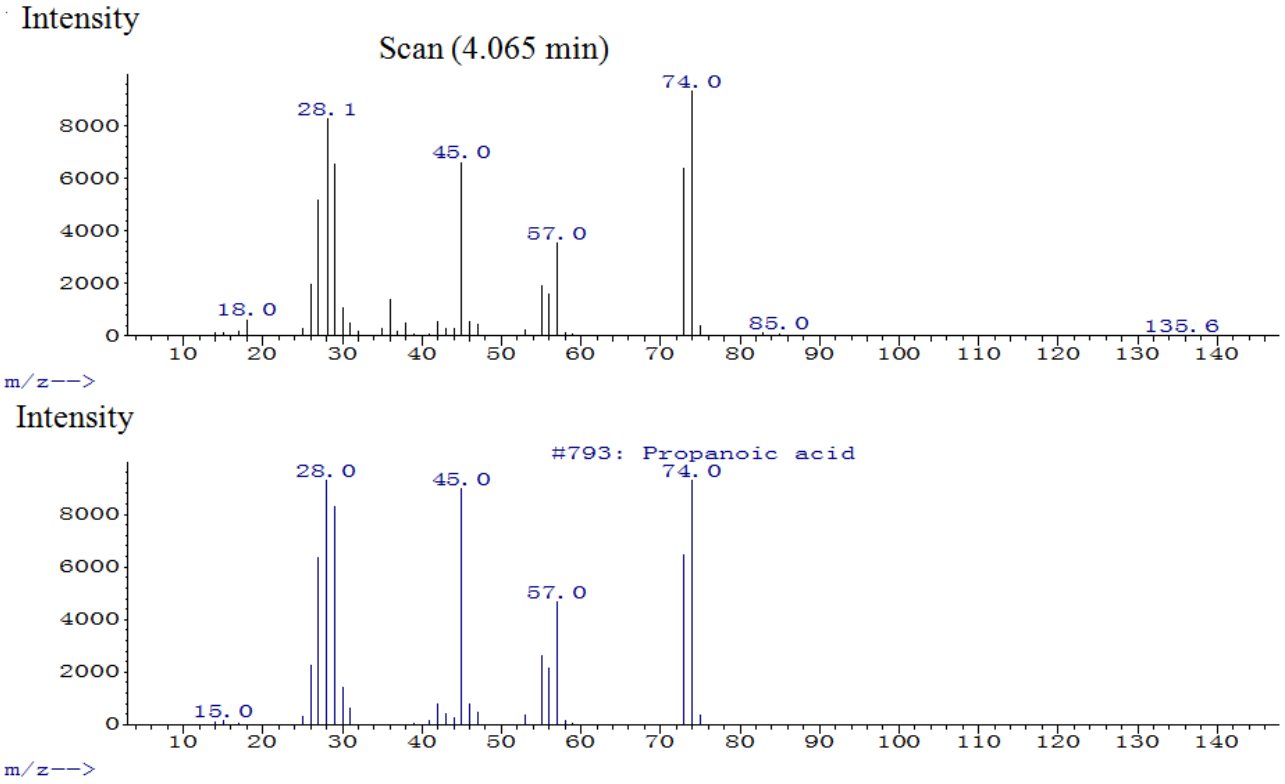

Figure S5-3. The Mass Spectra of propanoic acid in the permeate.

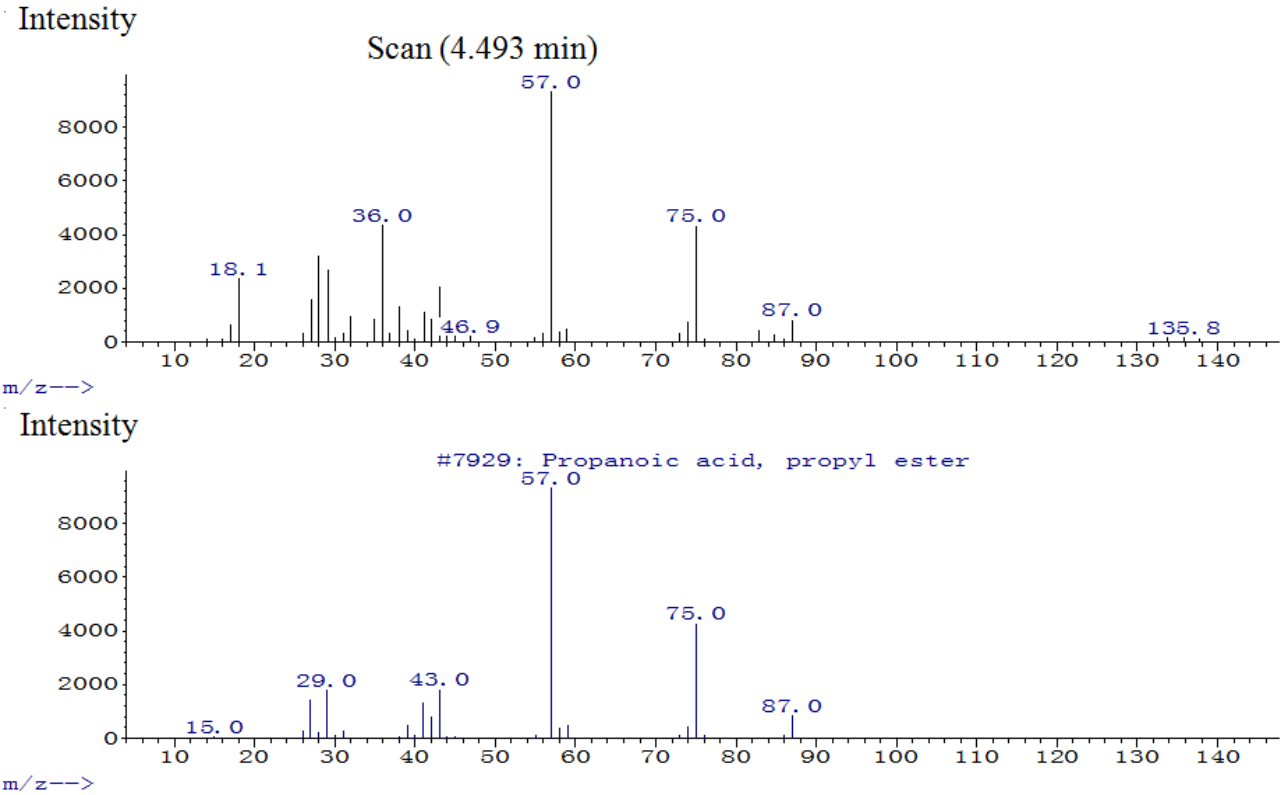

Figure S5-4. The Mass Spectra of propanoic acid, propyl ester in the permeate.

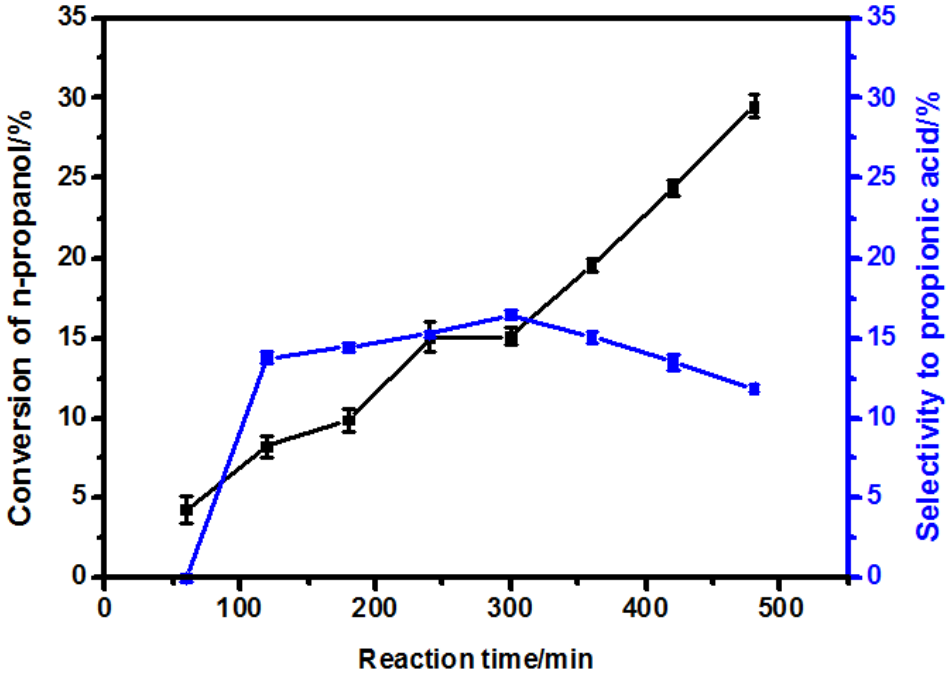

Figure S6. Conversion of n-propanol and selectivity to propionic acid versus reaction time in the reactor at the residence time of 0 min (namely a conventional electrocatalytic reactor with no permeate). The conversion of n-propanol increased from 4.31% to 29.5% with an increase in the reaction time from 0 to 480 min. The selectivity to propionic acid increased from 0 to 16.49% and then decreased to 11.88% during the reactor operation.

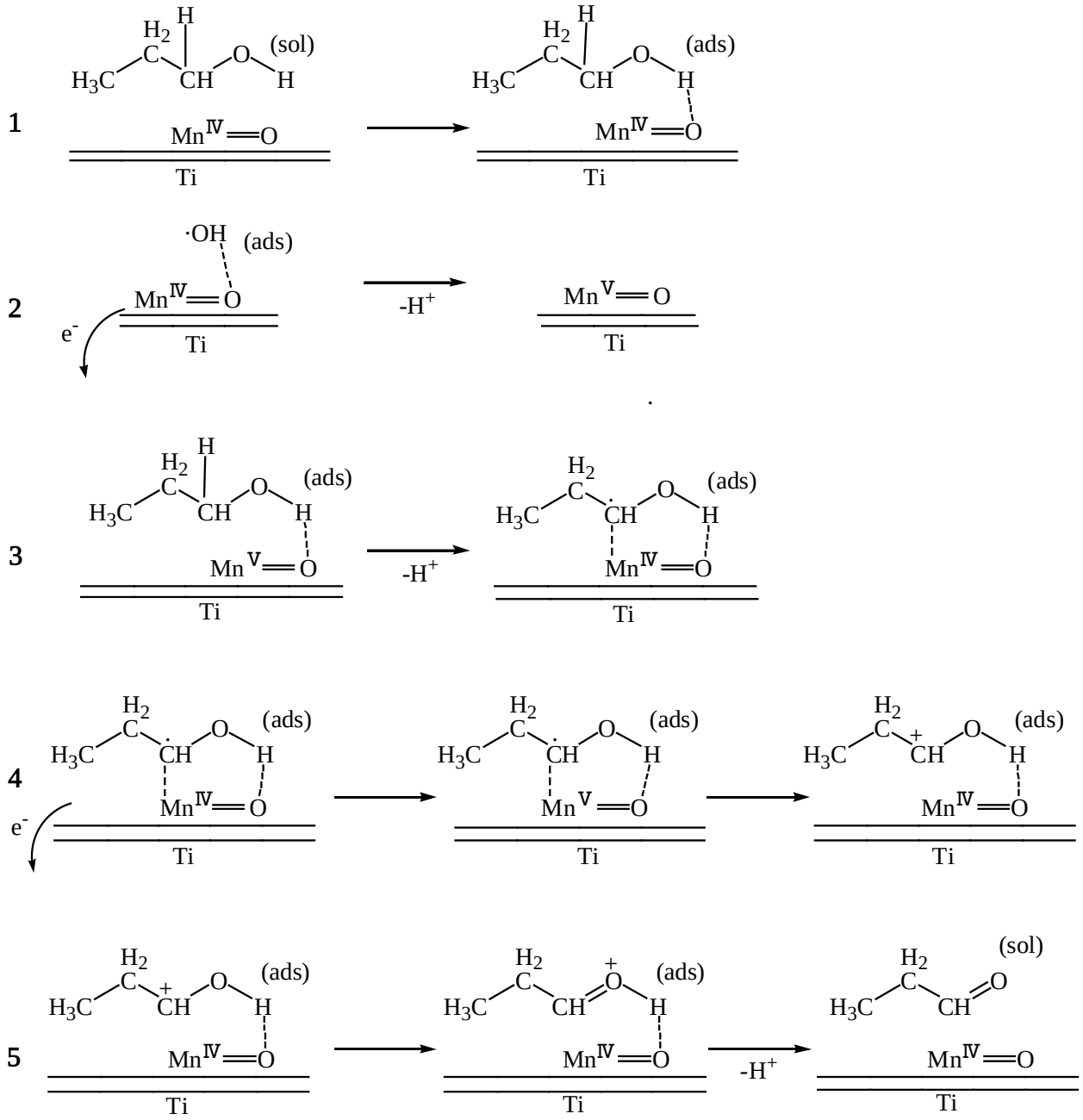
1
(sol)
(ads)
Mn^{IV}=O
Ti
2
·OH
(ads)
e$^-$
-H$^+$
Mn^{V}=O
3
(ads)
-H$^+$
4
(ads)
e$^-$
5
(ads)
(sol)
-H$^+$

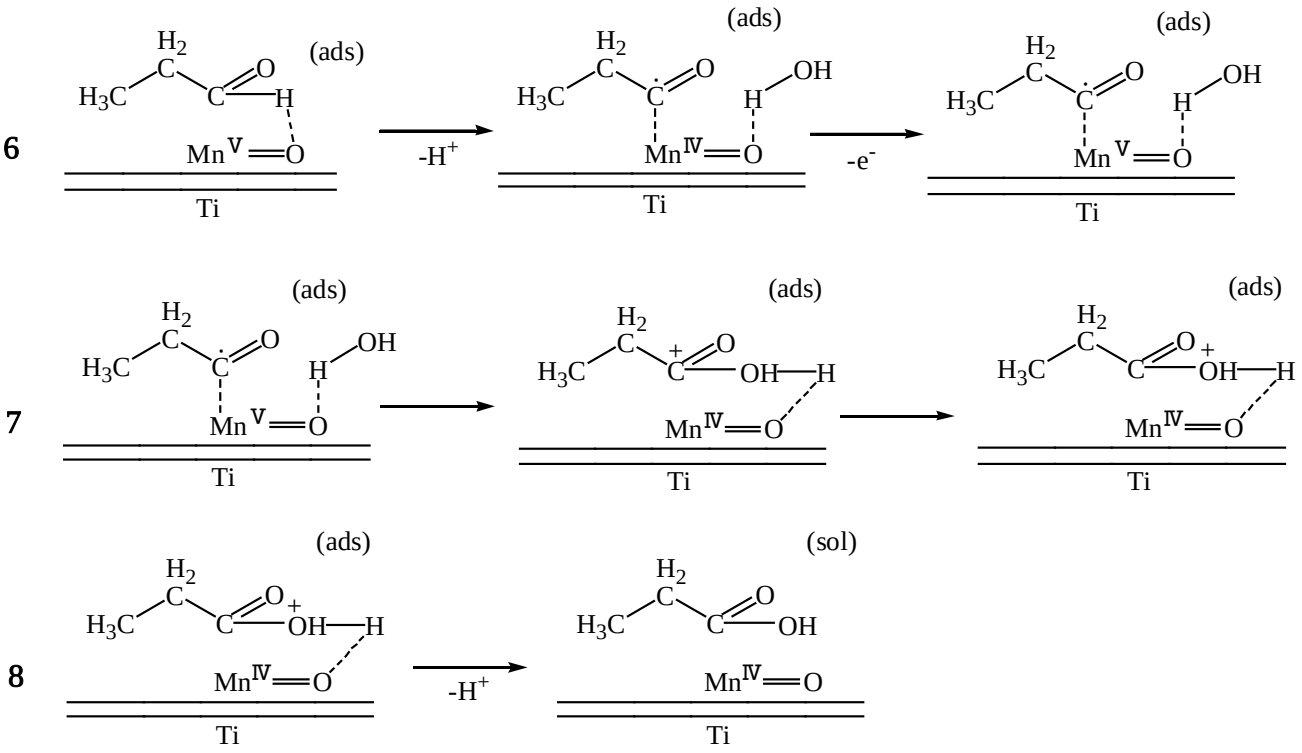

Figure S7. Proposed mechanism of electrochemical oxidation of n-propanol to produce propionic acid using MnO_2/Ti electrocatalytic membrane. Step 1 was the adsorption of n-propanol on the MnO_2/Ti electrocatalytic membrane surface. Step 2 was the oxidation of Mn (IV) to Mn (V) by hydroxyl radical. Steps 3 to 5 were the oxidation process of n-propanol to propanal through Mn (V) converted back to Mn (IV) by the redox reaction between Mn (V) and n-propanol. Steps 6 to 8 were the oxidation processes of propanal to propionic acid by means of the similar processes of the steps 3 to 5.

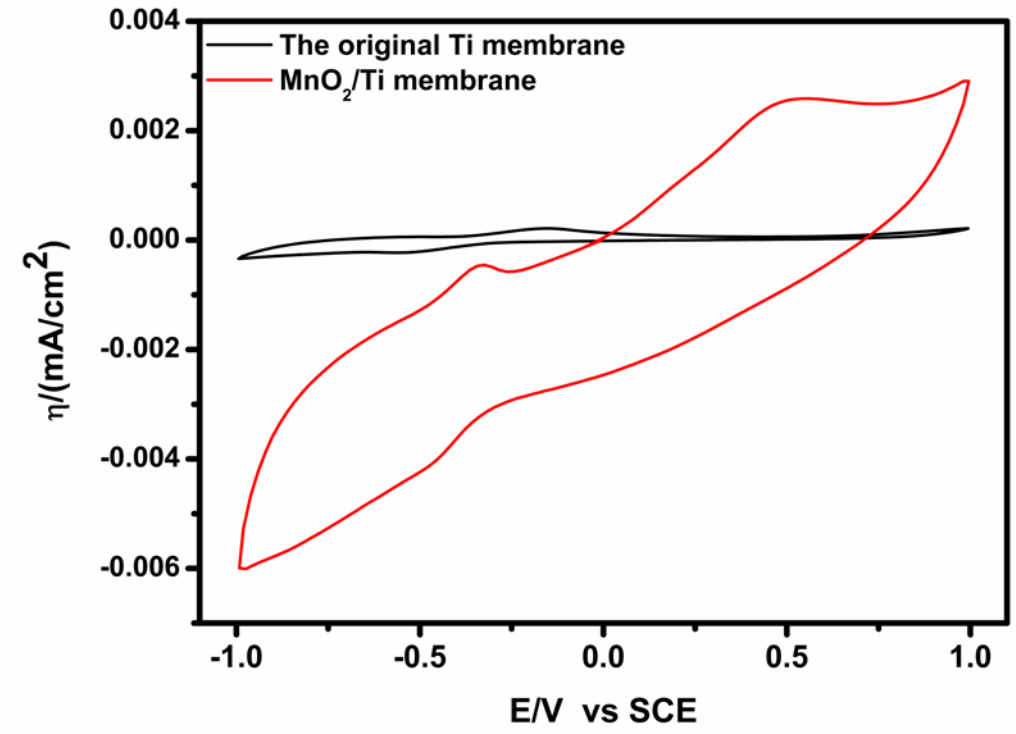

Figure S8. Cyclic voltammograms obtained in 0.1 M Na_2SO_4 solution at different membranes. Scan rate: 1 $mV \cdot s^{-1}$. It is found from Figure S9 that the current magnitude of CV from MnO_2/Ti membrane was much larger than that of the original titanium membrane. It implies that the MnO_2/titanium membrane electrode possesses a fast electron transfer process in this system. The oxidation peak at 0.5 V may attributed to the oxidation of Mn (IV) to Mn (V).[S5] There was no similar peak in the CV obtained from the original Ti membrane.

References:

[S1] Kennepohl, D.; Sanford, E. *Energ. Fuel.* **1996**, *10*, 229.

[S2] Furukawa, S.; Shishido, T.; Teramura, K.; Tanaka, T. *ACS Catal.* **2011**, *2*, 175.

[S3] Feng, Q.; Huang, K.; Liu, S.; Wang, X. *Electrochim. Acta.* **2010**, *55*, 5741.

[S4] a) Reddy, A. L. M.; Shaijumon, M. M.; Gowda, S. R.; Ajayan, P. M. *Nano Lett.* **2009**, *9*, 1002;

b) Chen, W.-M.; Qie, L.; Shao, Q.-G.; Yuan, L.-X.; Zhang, W.-X.; Huang, Y.-H. *ACS Appl. Mater. Inter.* **2012**, *4*, 3047.

[S5] Das, D.; Sen, P. K.; Das, K. *Electrochim. Acta.* **2008**, *54*, 289.